Monoalkyldecaborane(14) Syntheses via Nucleophilic Alkylation and Hydroboration

Adam N. Bridges, Douglas R. Powell, Joel A. Dopke, John M. Desper, and Donald F. Gaines*

Department of Chemistry, University of Wisconsin—Madison, Madison, Wisconsin 53706

Received September 5, 1997

Two regioselective, high-yield routes to *nido*-6-alkyldecaborane(14)s via one-pot syntheses are reported. Alkyllithium reagents add to salts of *nido*-$B_{10}H_{13}^-$ to form *arachno*-6-R-$B_{10}H_{13}^{2-}$, which may be protonated using HCl/Et_2O, first to the corresponding *arachno*-6-R-$B_{10}H_{14}^-$ anion and then, with H_2 loss, to *nido*-6-R-$B_{10}H_{13}$. Alternately, olefin hydroboration of *arachno*-6,9-$(SMe_2)_2$-$B_{10}H_{12}$ produces *nido*-6-R-8-(SMe_2)-$B_{10}H_{11}$, which may be reduced, using Superhydrid, to *nido*-6-R-$B_{10}H_{12}^-$, and then protonated with HCl/Et_2O to *nido*-6-R-$B_{10}H_{13}$. X-ray diffraction studies of the following intermediates and products are presented: *nido*-8-(SMe_2)-$B_{10}H_{12}$, *nido*-6-Thx-8-(SMe_2)-$B_{10}H_{11}$, and *nido*-6-Thx-$B_{10}H_{13}$.

Introduction

The regioselective, nucleophilic alkylation of *nido*-decaborane(14), $B_{10}H_{14}$, has until recently been difficult to achieve.

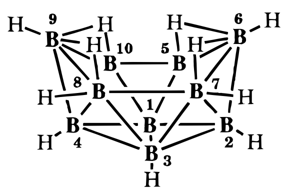

nido-$B_{10}H_{14}$

Most of the early reported alkylations produce mixtures of mono-, di-, and polyalkylation products and mixtures of isomers of each of the varieties, owing to a lack of understanding of the detailed reaction mechanisms and the conditions required for regioselective alkylations. Further, conditions that were found suitable for a given alkyl group were generally unsuitable for other alkyl groups. For example, reaction of ethyllithium with $B_{10}H_{14}$ to form 6-ethyl-$B_{10}H_{13}$ was reported to be quite successful,[1] but most other alkyllithium reagents produced mixtures of 5- and 6-alkyl-$B_{10}H_{13}$, as well as multialkylated derivatives. The early literature implied that alkyllithium reagents form intermediate R-$B_{10}H_{14}^-$ type species, which on acidification produced alkylated products. We found, however, that a multitude of reactions occur, and the nature of the alkyl group and the reaction conditions altered the complexity of the reactions. The reactions were therefore not considered suitable for regioselective monoalkylation.

Grignard-type reactions have likewise proved complex. Decaborane(14) reacts with methyl- or ethylmagnesium iodide to form $B_{10}H_{13}$MgI (major product), along with the 6-Me- or 6-Et-$B_{10}H_{13}$, respectively. $B_{10}H_{13}$MgI reacts with triethyloxonium tetrafluoroborate or diethyl sulfate to form 5-ethyldecaborane and with dimethyl sulfate to form a 1:1 mixture of 5- and 6-methyldecaborane. Benzyl chloride reacts with $B_{10}H_{13}$MgI to form 6-benzyldecaborane.[2] $B_{10}H_{13}$MgI appears to not react with alkyl chlorides, bromides, or iodides but does react with allyl bromide[3] and with alkyl fluorides[4] to form the corresponding allyl- and alkyl decaboranes, though the alkylation sites are not known.

Reactions of the $B_{10}H_{13}^-$ anion with dimethyl or diethyl sulfate and with benzyl chloride also produce 6-alkyldecaboranes.[5] This appears not to be a general reaction, requiring strong electrophiles for satisfactory results.[6,7]

Insertion of a phenylborane moiety into a B_9 anion has been used to form 6-phenyldecaborane,[8] though the reaction has yet to be shown to be generally applicable.

A recently described route to 6-X-$B_{10}H_{13}$, where X = phenyl, cyclohexyl, or triflate($CF_3SO_3^-$), via reaction of *closo*-$B_{10}H_{10}^{2-}$ with triflic acid in the presence of benzene or cyclohexane likely occur via protonation to a $B_{10}H_{13}^+$ (22-e$^-$) electrophile and subsequent electrophilic substitution of an arene or activation of an alkane C−H bond, a previously unprecedented process in borane cluster chemistry.[9]

Quite efficient transition metal halide catalyzed hydroborations using $B_{10}H_{14}$ have also been recently described. In these syntheses chloroplatinic acid or platinum(II) bromide catalyze reactions of $B_{10}H_{14}$ with terminal olefins to produce the corresponding 6,9-$R_2B_{10}H_{12}$ derivatives in high yields.[10]

In the course of other investigations of decaborane chemistry, we undertook explorations of nucleophilic attack on the decaborane framework, which in turn necessitated the synthesis of isomerically pure 6-alkyl-$B_{10}H_{13}$ derivatives. Herein we report two high-yield routes to 6-alkyl-decaboranes.[11] Also included for comparison purposes, as an appendix, are the x-ray determined structures of *nido*-8-(SMe_2)-$B_{10}H_{12}$, *nido*-6-Thx-8-(SMe_2)-$B_{10}H_{11}$, and *nido*-6-Thx-$B_{10}H_{13}$.

(1) Williams, R. L.; Dunstan, I.; Blay, N. J. *J. Chem. Soc.* **1960**, 5012.
(2) (a) Williams, R. L.; Dunstan, I.; Blay, N. J. *J. Chem. Soc.* **1960**, 5016. (b) Siegel, B.; Mack, J. L.; Lowe, J. V.; Gallaghan, J. *J. Am. Chem. Soc.* **1958**, *80*, 4523.
(3) Cueilleron, J.; Guillot, P. *Bull. Soc. Chim. Fr.* **1960**, 2044.
(4) Gallaghan, J.; Siegel, B. *J. Am. Chem. Soc.* **1959**, *81*, 504.
(5) Blay, N. J.; Pace, R. S.; Williams, R. L. *J. Chem. Soc.* **1962**, 3416.
(6) Palchak, R. J. F.; Norman, J. H.; Williams, R. E. *J. Am. Chem. Soc.* **1961**, *83*, 3380.
(7) Plzak, Z.; Stibr, B.; Plesek, J.; Hermanek, S. *Coll. Czech. Chem. Commun.* **1975**, *40*, 3602.
(8) McDowell, D.; Siedle, A. R.; Todd, L. J. *Inorg. Chem.* **1974**, *13*, 2735.
(9) Hawthorne, M. F.; Mavunkal, I. J., Knobler, C. B. *J. Am. Chem. Soc.* **1992**, *114*, 4427−29.
(10) Mazighi, K.; Carroll, P. J.; Sneddon, L. G. *Inorg. Chem.* **1993**, *32*, 1963.
(11) Bridges, A. N.; Gaines, D. F. *Organometallics* **1993**, *12*, 2015−2016.

S0020-1669(97)01149-X CCC: $15.00
Published on Web 01/22/1998

Results and Discussion

6-Alkyldecaborane Syntheses via Alkyllithium Reagents. Alkyllithium Addition to $B_{10}H_{13}^-$: Formation of 6-R-$B_{10}H_{13}^{2-}$. While the reaction of alkyllithium compounds with $B_{10}H_{14}$ are generally very complex, reaction of alkali metal salts of $B_{10}H_{13}^{-1}$ with RLi (MeLi, *n*-BuLi, *t*-BuLi, and PhLi) in Et_2O produce colorless, sparingly soluble *arachno*-6-R-$B_{10}H_{13}^{2-}$ salts quantitatively, based on ^{11}B NMR analysis. Alternatively, addition of an alkyllithium to tetraalkylammonium salts[12] of $B_{10}H_{13}^-$ can be conducted in THF. Tetraalkylammonium/lithium salts of the R-$B_{10}H_{13}^{2-}$ products appear to be more robust than their alkali metal/Li counterparts. The most nonpolar solvent available should be used if isolation of intermediate products is required. For example, (Na,Li)[6-R-$B_{10}H_{13}$] species in Et_2O often form an uncharacterized, intractable, gelatinous solid on standing. The (R_4N^+,Li^+) salts of 6-R-$B_{10}H_{13}^{2-}$ are somewhat more soluble in THF and can be precipitated by the addition of Et_2O.

Protonation of 6-R-$B_{10}H_{13}^{2-}$: Formation of 6-R-$B_{10}H_{14}^-$. Protonation of the sparingly soluble 6-R-$B_{10}H_{13}^{2-}$ species with 1 equiv of 1.0 M HCl/Et_2O produces the 6-R-$B_{10}H_{14}^-$ salt and a white precipitate (most likely LiCl). When the tetraalkylammonium/Li derivatives of 6-R-$B_{10}H_{13}^{2-}$ are used, ^{1}H NMR spectra confirm the presence of the R_4N^+ counterion in the 6-R-$B_{10}H_{14}^-$ (R = Me, Et) product.

Protonation of 6-R-$B_{10}H_{14}^-$: Formation of 6-R-$B_{10}H_{13}$. Protonation of the 6-R-$B_{10}H_{14}^-$ monoanion, immediately after its formation, with an additional equivalent of 1.0 M HCl/Et_2O produces additional white solid and gas evolution. ^{11}B NMR analysis of the reaction solution indicates exclusive formation of 6-R-$B_{10}H_{13}$. If the 6-R-$B_{10}H_{14}^-$ monoanion is allowed to remain in solution for some time, a new lower symmetry species begins to form, and subsequent protonation with HCl/Et_2O yields 5-R-$B_{10}H_{13}$ in addition to the primary product, 6-R-$B_{10}H_{13}$. The formation of the 5-R-$B_{10}H_{13}$ derivative in the product likely results from slow isomerization of 6-R-$B_{10}H_{14}^-$ to 5-R-$B_{10}H_{14}^-$.

One-Pot Synthesis of 6-R-$B_{10}H_{13}$ by the Alkyllithium Route. The above steps can be combined to produce a convenient "one-pot" synthesis of *nido*-6-R-$B_{10}H_{13}$ derivatives. Three factors governing the success of this sequence are solvent, choice of cation, and the potential for isomerization of the intermediate, 6-R-$B_{10}H_{14}^-$. In the first step, the addition of RLi to $B_{10}H_{13}^-$, an excess of RLi can be used as the excess is consumed during the subsequent addition of acid. The partially soluble product, MLi[6-R-$B_{10}H_{13}^{2-}$] (M = Na, R_4N), appears to be quite stable in solution. Subsequent protonation with an excess of 2 equiv of HCl/Et_2O results in loss of hydrogen and formation of the *nido*-6-R-$B_{10}H_{13}$. The use of the specified cations is important to achieve clean elimination of the salts and to prevent side reactions.

6-Alkyldecaborane Syntheses via Olefin Hydroboration Using 6,9-$(SMe)_2$-$B_{10}H_{12}$. Tolpin *et al*. reported the first hydroboration of an olefin using the bis-adduct of decaborane 6,9-$(SMe)_2$-$B_{10}H_{12}$ and cyclohexene to form *nido*-6-Cy-8-SMe_2-$B_{10}H_{11}$ (Cy = cyclohexyl).[13] We have modified the original reaction conditions to allow high yield syntheses of a variety of *nido*-6-R-8-SMe_2-$B_{10}H_{11}$ derivatives. Subsequent conversion to 6-R-$B_{10}H_{12}^-$ anions using Superhydride, Li[Et_3BH]/THF, followed by anhydrous protonation produces the neutral 6-R-$B_{10}H_{13}$. The combination of these reactions results in another "one-pot" synthesis route for 6-R-$B_{10}H_{13}$.

(12) Hawthorne, M. F.; Pitochelli, A. R., Strahm, R. D., Miller, J. J. *J. Am. Chem. Soc.* **1960**, *82*, 1825−9.
(13) Dupont, J. A.; Hawthorne, M. F. *Chem. Ind.* **1962**, 405.

Table 1. Reaction Conditions for 6-R-8-SMe_2-$B_{10}H_{11}$ Syntheses

Olefin	Reaction Conditions	Product
propene	sealed vacuum; room temp. CH_2Cl_2; 4 days	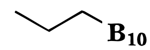
1-hexene	under N_2; room temp. CH_2C_2; 2 days	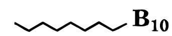
1-octene	under N_2; reflux temp. benzene; 3.5 hrs.	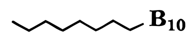
2,3-dimethyl-1-butene	under N_2; room temp. CH_2Cl_2; 2 days	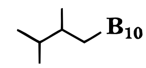
2-methyl-2-butene	under N_2; room temp. CH_2Cl_2; 3 days	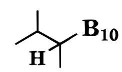
2,3,dimethyl-2-butene	under N_2; room temp CH_2Cl_2;4 days	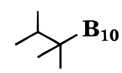

Olefin Hydroboration Using 6,9-$(SMe)_2$-$B_{10}H_{12}$: Synthesis of 6-R-8-SMe_2-$B_{10}H_{11}$. We found that the hydroboration of olefins via 6,9-$(SMe)_2$-$B_{10}H_{12}$ occurs at an acceptable rate at room temperature in CH_2Cl_2, producing 6-R-8-SMe_2-$B_{10}H_{11}$ in very high yield. However, for room-temperature reactions two factors are important: use of a 3- to 4-fold excess of alkene and removal of the liberated dimethyl sulfide. Reactions of 6,9-$(SMe)_2$-$B_{10}H_{12}$ were carried out with propene, 1-hexene, 1-octene, 2-methyl-2-butene, 2,3-dimethyl-1-butene, and 2,3-dimethyl-2-butene to explore the influence of steric hindrance on reaction times and to determine whether the reaction was always regiospecific. Reaction conditions and product identities are shown in Table 1. The reactions can be conducted in aromatic hydrocarbons at elevated temperatures,[13] but above ca. 85 °C significant amounts of 8-SMe_2-$B_{10}H_{12}$ form. The rates of hydroboration are affected by the steric hindrance of the olefin. At room temperature, reactions with primary olefins, such as 1-hexene and 1-octene, generally go to completion within 1 day. Reactions with secondary olefins, such as 2-methyl-2-butene and 2,3-dimethyl-1-butene, take between 2 and 3 days, while tertiary olefins, such as 2,3-dimethyl-2-butene, require up to 4 days. Gaseous olefins, propene for example, require a sealed environment, and as there is no avenue for Me_2S escape, the reaction takes considerably longer. In this case periodic venting of the system followed by replacement of the olefin is necessary for complete reaction. Other experiments have shown that hydroboration reaction rates are substantially slower when additional Me_2S is present.

The *nido*-6-R-8-SMe_2-$B_{10}H_{11}$ products can be isolated by vacuum removal of volatile olefins or by chromatographic removal of the olefin by elution with hexanes, followed by elution of the 6-R-8-SMe_2-$B_{10}H_{11}$ with a CH_2Cl_2/hexanes mixture. Although the 6-R-8-SMe_2-$B_{10}H_{11}$ compounds are recovered in high purity by these procedures, they are typically clear viscous oils that slowly discolor upon standing. Accurate determination of yields is difficult in some cases owing to solvent retention. Long-term exposure to air leads to formation of gelatinous solids insoluble in CH_2Cl_2 and aromatic hydrocarbons.

Hydridic Reduction of 6-R-8-SMe$_2$-B$_{10}$H$_{11}$ to 6-R-B$_{10}$H$_{12}^-$ and Subsequent Protonation to 6-R-B$_{10}$H$_{13}$. Conversion of 6-R-8-SMe$_2$-B$_{10}$H$_{11}$ to the neutral 6-alkyldecaborane(14), 6-R-B$_{10}$H$_{13}$, requires a reaction to remove the Me$_2$S group. We found that Superhydride, Li[Et$_3$BH]/THF, converts 6-R-8-SMe$_2$-B$_{10}$H$_{11}$ to bright yellow solutions of the 6-R-B$_{10}$H$_{12}^-$ anion. Whether the incoming hydride directly displaces the Me$_2$S group or attacks another location followed by rearrangement and release of Me$_2$S is yet to be determined.

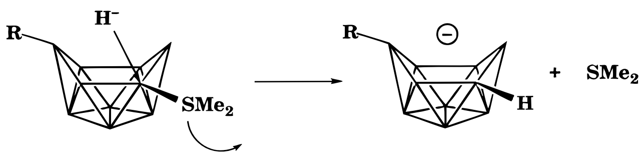

Subsequent addition of 1 molar equiv of HCl/Et$_2$O discharges the yellow color, precipitates a white solid (presumably LiCl), and converts the anion to the corresponding neutral *nido*-6-R-B$_{10}$H$_{13}$ in high yield, based on ^{11}B NMR.

The addition of 2 molar equiv of Li[Et$_3$BH]/THF to the 6-R-8-SMe$_2$-B$_{10}$H$_{11}$ derivatives produces 6-R-B$_{10}$H$_{13}^{2-}$ derivatives. Sodium superhydride, Na[Et$_3$BH]/toluene, is a more powerful hydride source than Li[Et$_3$BH]/THF and could not be controlled to produce *nido*-6-R-B$_{10}$H$_{12}^-$. Instead, 1 molar equiv of Na[Et$_3$BH]/toluene produces 0.5 an equiv of the *arachno*-6-R-B$_{10}$H$_{13}^{2-}$ derivative.

One-Pot Synthesis of 6-R-B$_{10}$H$_{13}$ via the Hydroboration Route. A convenient, high-yield, one-pot route to *nido*-6-R-B$_{10}$H$_{13}$ compounds is achieved by omitting the isolation of intermediates in the hydroboration transformations. A typical synthesis is that of *nido*-6-Thx-B$_{10}$H$_{13}$. In this synthesis the slow step is the hydroboration of the olefin, 2,3-dimethyl-2-butene, with the limiting reagent, 6,9-(SMe)$_2$-B$_{10}$H$_{12}$. This step is monitored periodically by ^{11}B NMR to ensure complete conversion. The hydroboration must be complete before addition of the Li[Et$_3$BH]/THF to avoid its reaction with 6,9-(SMe)$_2$-B$_{10}$H$_{12}$.

After hydroboration, the excess 2,3-dimethyl-2-butene is removed by evaporation in vacuum. The 6-Thx-8-SMe$_2$-B$_{10}$H$_{11}$-(8)-SMe$_2$ product is dissolved in CH_2Cl_2 and treated with a stoichiometric amount of Li[Et$_3$BH]/THF. A bright-yellow color signals reduction. Immediately following the reduction an excess of 1.0 M HCl/Et$_2$O is added (excess acid will ensure that any residual Li[Et$_3$BH]/THF is quenched.). The yellow color fades and a white precipitate forms. At this point two boron products, Et$_3$B and 6-Thx-B$_{10}$H$_{13}$, are observable by ^{11}B NMR. The mixture is filtered to remove LiCl, and the Et$_3$B and solvents are vacuum evaporated overnight to leave a high yield of 6-Thx-B$_{10}$H$_{13}$, which often crystallizes upon standing.

We have used high-vacuum microdistillation and rotary chromatography for purification of 6-R-B$_{10}$H$_{13}$ compounds. The former method is quicker, more convenient, and generally produces a cleaner appearing product, but yields are lower, possibly owing to thermal decomposition. For rotary chromatography, the reaction residue is applied to the plate as a CH_2Cl_2 solution under nitrogen, evaporated, and then eluted with hexanes. A light-yellow product is recovered, though ^{1}H and ^{13}C NMR spectra do not indicate detectable impurities. The purified 6-alkyldecaboranes are moderately air-sensitive but can be handled in air for brief periods. A general overview of the two routes to 6-R-B$_{10}$H$_{13}$ derivatives is presented in Scheme 1.

Scheme 1. Synthetic Routes to 6-R-B$_{10}$H$_{13}$

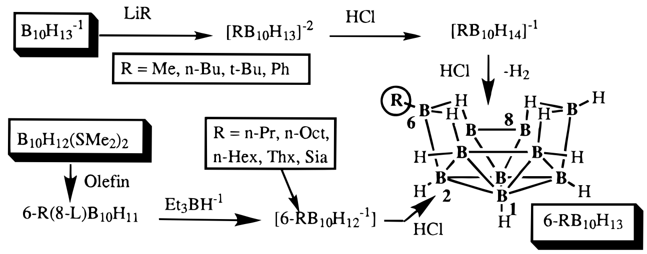

NMR and Structural Characterization. ***arachno*-6-R-B$_{10}$H$_{13}^{2-}$.** The ^{11}B NMR spectra of *arachno*-6-R-B$_{10}$H$_{13}^{2-}$ derivatives are as expected on the basis of the parent *arachno*-B$_{10}$H$_{14}^{2-}$ dianion.[14] The spectrum of 6-Me-B$_{10}$H$_{13}^{2-}$, for example (Supporting Information Figure S1), consists of six signals in a ratio of 1:1:2:3:2:1 and is symmetrically consistent with a 6-substituted-decaborane cage (assuming one coincident resonance). The triplet of intensity one at −39.7 ppm and the absence of any singlet resonances in this spectrum are consistent with that expected for an *arachno*-6-substituted B$_{10}$H$_{14}^{2-}$ structure with a B(R)H at B(6), BH$_2$ at the B(9), and bridging hydrogens spanning the B(7,8) and B(5−10) positions. The broadened nature of several of the resonances precluded the use of ^{11}B−^{11}B COSY NMR to determine assignments, but the spectrum can be compared to the known *arachno*-decaborane derivative 6-CN-B$_{10}$H$_{13}^{2-}$,[15] the resonances of which have been assigned using ^{11}B−^{11}B COSY NMR (Supporting Information Figures S2 and S3). The broadened doublet at $^{2-}$1.0 ppm is assigned to the substituted B(6) signal, but the *endo* or *exo* location of the substituent is undetermined. The ^{11}B NMR resonances for the methyl and *n*-butyl derivatives appear to be similar in chemical shift, but there are some notable perturbations in the *tert*-butyl derivative, where the B(6) and B(9) signals are shifted downfield by 6 ppm, while the B(2) resonance is shifted upfield by 6 ppm. ^{11}B NMR data for the various 6-R-B$_{10}$H$_{13}^{2-}$ derivatives are tabulated in Table 1.

***arachno*-6-R-B$_{10}$H$_{14}^{-1}$.** The ^{11}B NMR spectra of the 6-R-B$_{10}$H$_{14}^{-1}$ derivatives are similar to that of the parent species B$_{10}$H$_{15}^-$ (prepared by the protonation of B$_{10}$H$_{14}^{2-}$)[16] and are radically different from those of the precursor *arachno*-6-R-B$_{10}$H$_{13}^{2-}$ dianion. The resonances of 6-R-B$_{10}$H$_{14}^-$, in a ratio of 1:2:2:1:2:2, appear in a very narrow region of the spectrum, and the apparent symmetry is consistent with a 6-substituted arrangement. In the methyl derivative, the substituted resonance is obscured, but in both the *n*-Bu- and *t*-Bu derivatives, the substituted signal is shifted downfield enough to be observed. A 6-substituted decaborane system would be expected to possess *four* single intensity resonances, so the appearance of higher symmetry may be the result of considerable coincidental overlap or rapid internal exchange. The ^{11}B−^{11}B COSY NMR spectrum of 6-*n*-Bu-B$_{10}$H$_{14}^-$ (Supporting Information Figure S5) provides partial connectivity information, and appears consistent with a 6-substituted decaborane structure. ^{11}B NMR data for the 6-R-B$_{10}$H$_{14}^-$ derivatives are tabulated in Table 2.

***nido*-6-R-8-SMe$_2$-B$_{10}$H$_{11}$.** The structure of 6-Cy-8-SMe$_2$-B$_{10}$H$_{11}$ has previously been determined and numbered.[13,17] As

(14) Muetterties, E. L. *Inorg. Chem.* **1963**, *2*, 647−8.
(15) (a) Knoth, W. H.; Muetterties, E. L. *J. Inorg. Nucl. Chem.* **1961**, *20*, 66−72. (b) Knoth, W. I., Muetterties, E. L. *Inorg. Chem.* **1965**, *4*, 1498−9.
(16) Tolpin, E. I.; Mizusawa, E.; Scott-Becker, D.; Venzel, J. *Inorg. Chem.* **1980**, *19*, 1182.
(17) Venable, T. L.; Hutton, W C.; Grimes, R. N. *J. Am. Chem. Soc.* **1984**, *106*, 29.

Table 2. ^{11}B NMR Data for 6-R-$B_{10}H_{13}^{2-}$ and 6-R-$B_{10}H_{14}^{-}$ Derivatives[a]

	Me-	*n*-Bu-	*t*-Bu-
		6-R-$B_{10}H_{13}^{2-}$	
B(2)	+1.5 d (127)	+0.5 d (115)	−5.8 d (104)
B(4)	−3.3 d (103)	−5.1 d (132)	−7.1 d (104)
B(5,7)	−16.8 d (113)	−17.8 br (−)	−18.8 br (−)
B(6)	−21.0 d (br.)	−26.4 d (104)	−12.1 d (86)
B(8,10)	−21.4 d (br.)	−23.0 br (−)	−18.8 br (−)
B(1,3)	−37.3 d (137)	−39.0 d (138)	−39.7 d (116)
B(9)	−39.7 t (112)	−40.9 t (92)	−36.5 t (81)
	Et_2O; 160 MHz; Na^+, Li^+	THF; 115 MHz; Me_4N_+, Li^+	THF; 115 MHz; Me_4N^+, Li^+
		6-R-$B_{10}H_{14}^{-}$	
B(6)	−20.5 s (−)	−9.7 s (−)	−6.2 s (−)
B(5,7)	−11.6 d (144)	−12.3 d (136)	−13.4 d (120)
B(8,10)	−13.6 d (136)	−14.0 d (132)	−14.5 d (132)
B(2)	−17.8 d (152)	−18.6 d (137)	−19.9 d (126)
B(1,3)	−20.5 d (144)	−20.6 d (141)	−21.0 d (144)
B(4,9)	−22.2 d (br.)	−22.1 d (127)	−22.4 d (126)
	THF; 160 MHz; Na^+	THF; 160 MHz; Me_4N^+	THF; 115 MHz; Me_4N^+

[a] Coupling constants are in parentheses. Solvent, NMR frequency, and counterions appear below each column.

the objective of our chemistry was the alkylation of decaborane(14), we have altered the numbering scheme for these derivatives to reflect this priority, as shown for one enantiomorph:

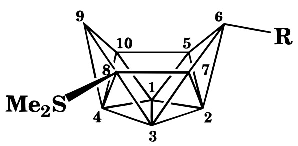

The 115 MHz ^{11}B NMR spectra of the 6-R-8-SMe_2-$B_{10}H_{11}$ compounds are quite similar to that of the original 6-Cy-8-SMe_2-$B_{10}H_{11}$[13] and are tabulated in Table 3. A typical example is 6-Thx-8-SMe_2-$B_{10}H_{11}$, whose spectrum consists of 10 signals of intensity one. Individual resonances exhibit varying degrees of broadening. The region between +5 and −5 ppm contains five resonances, some overlapping. The Me_2S-substituted B(8) singlet is located at +0.4 ppm. The major difference between the parent 8-SMe_2-$B_{10}H_{12}$ and 6-Thx-8-SMe_2-$B_{10}H_{11}$ is the downfield shift of the Thx-B(6) resonance, which appears as a singlet at +11.7 ppm. The B(6) resonance is the only signal that differs significantly in each derivative. The downfield resonance at +19.0 ppm is quite broad. The assignments of the resonances are based in part on similarities to the ^{11}B NMR spectrum of the parent compound, 8-SMe_2-$B_{10}H_{12}$, and in part on the basis of ^{11}B−^{11}B COSY NMR spectra. While all expected connectivities were not observed in the ^{11}B−^{11}B COSY NMR spectra, sufficient information was obtained to unambiguously assign all resonances. The absence of cross-coupling between B(6) and both B(5) and B(7) and between B(9) and B(10) suggests that the bridging hydrogens span the B(5)−B(6), B(6)−B(7), and B(9)−B(10) vertices, as their presence often disturbs the magnetization directed along a B−B connectivity.[17] This conclusion is consistent with the solid state structure of 6-Cy-8-SMe_2-$B_{10}H_{11}$[18] and our determination of the 8-SMe_2-$B_{10}H_{12}$ structure, shown below.

^{1}H NMR in combination with ^{13}C NMR and DEPT-135 ^{13}C NMR were utilized to determine the hydrocarbon structures in the 6-R-8-SMe_2-$B_{10}H_{11}$ compounds. Two aspects of both ^{1}H and ^{13}C spectra were observed in all derivatives: two resonances arising from the Me_2S group and a broadened hump in the ^{13}C NMR corresponding to the α-carbon adjacent to the boron cage. In CD_2Cl_2 resonances for the Me_2S group appear at +2.66 and +2.68 ppm in the ^{1}H NMR spectrum and at +25.6 and +27.8 ppm in the ^{13}C NMR spectrum. These carbon resonances are shifted upfield to +22.7 and +25.0 ppm in C_6D_6. Only one hydrocarbon structure, that of the anticipated anti-Markovnikov product, was observed for each derivative.

In a number of the derivatives many of the carbon resonances appeared to be split into two resonances, suggesting asymmetry or the presence of two distinct but related species. That this is not observed in the neutral 6-R-$B_{10}H_{13}$ derivatives suggests that the Me_2S group is responsible. Tolpin[16] had ascribed the presence of two Me_2S resonances in 6-Cy-8-SMe_2-$B_{10}H_{11}$ to an isomerism generated by a barrier to rotation in the B−S bond, and a theoretical energy diagram based on rotation of the Me_2S group upon its B−S axis was developed. It is our view, however, that the two signals observed for the Me_2S group are not a result of a rotational barrier but because the attachment of the sulfur atom to the asymmetric cage structure does not permit the two methyl groups to be equivalent at any time. Not all of the spectra display two signals for each carbon atom, and for some derivatives the downfield Me_2S resonance is split into two signals. One derivative, 6-Sia-8-SMe_2-$B_{10}H_{11}$, displays asymmetry in the B(7) position at −13 ppm in the ^{11}B NMR spectrum. The area of this signal is still only 1B, suggesting that in this derivative the rotamer effect produces a large electronic difference in the B(7) signal. The thexyl derivative does not display this asymmetry in the B(7) position, and we feel that a rotamer argument is insufficient to account for the above observations.

We conclude, therefore, that the ^{13}C NMR spectra of both 6-Sia-8-SMe_2-$B_{10}H_{11}$ and 6-Thx-8-SMe_2-$B_{10}H_{11}$ are a result of diastereoisomerism generated by the presence of the chiral centers in the alkyl group and the B_{10} cage. Figure 1 displays the possible diastereomers for the siamyl, thexyl, and 2,3-dimethyl-1-butyl groups. The inequivalence of all carbons in each alkyl moiety results from the presence of the dimethyl sulfide group on one side of the cage. The number of sharp carbon resonances observed is always one less than the actual number owing to the broad nature of the α-carbon. The duplication of each of the resonances in the siamyl derivative is the result of the chiral α-carbon center which generates two diastereomers with slightly different chemical shifts. This is not observed in the case of the achiral thexyl derivative. Diastereomers are also observed in the 2,3-dimethyl-1-butyl derivative, where chirality exists at the *β*-carbon. However, in this case some chemical shifts appear to be coincident. Another indication of the formation of diastereomers is seen in the ^{1}H and ^{13}C NMR resonances of the methyl groups on the sulfur atom. Although four resonances are presumed to be present, only the downfield signal shows different chemical shifts, likely a result of that carbon's proximity to the other chiral center. This is a reasonable assumption given that the chemical shift difference is more pronounced in the siamyl derivative, where the chiral center is at the α-carbon.

In derivatives where two diastereomers are generated, two sets of 10 ^{11}B NMR resonances should be observed. In most cases, however, the small chemical shift differences prevents their observation. In the siamyl derivative two signals appear for the B(7) resonance, all other resonances being coincident.

Let us consider the question of how the 6-R-8-SMe_2 -$B_{10}H_{11}$ forms. The major transitions in this reaction are the loss of one Me_2S from the cage, the regiospecific, anti-Markovnikov

(18) Mizusawa, E.; Rudnick, S. E.; Eriks, K. *Inorg. Chem.* **1980**, *19*, 1188.

Table 3. ^{11}B NMR Data for 6-R-8-SMe_2-$B_{10}H_{11}$ Derivatives[a]

x for B(*x*)	*n*-Hex-	*n*-Oct-	2,3-dimethyl-1-butyl-	Sia-	Thx-
9	+19.4 (br)	+19.2 (br)	+19.4 (br)	+19.3 (br)	+19.0 (br)
6	+9.4 (-)	+9.5 (-)	+9.1 (-)	+10.3 (-)	+11.7 (-)
3	+4.4 (137)	+4.5 (137)	+5.0 (144)	+4.5 (136)	+4.4 (137)
5	+0.3 (-)	+0.3 (-)	0.0 (-)	−0.1 (-)	+0.4 (-)
8	+0.3 (br)	+0.3 (br)	0.0 (br)	−0.1 (br)	+0.4 (br)
10	−4.7 (136)	−4.6 (128)	−3.8 (120)	−4.5 (136)	−4.6 (137)
1	−6.0 (152)	−5.9 (141)	−5.0 (136)	−5.4 (147)	−5.8 (146)
7	−13.0 (103)	−13.0 (122)	−12.4 (120)	−13.1 (128)	−13.5 (137)
4	−31.3 (141)	−31.3 (141)	−30.8 (136)	−31.3 (144)	−31.4 (142)
2	−40.3 (146)	−40.2 (152)	−39.6 (152)	−40.7 (147)	−41.0 (147)
	CD_2Cl_2; 160 MHz	CD_2Cl_2; 160 MHz	C_6D_6; 160 MHz	CD_2Cl_2; 160 MHz	CH_2Cl_2; 115 MHz

[a] Coupling constants are in parentheses. Solvents and ^{11}B NMR frequencies are at the bottom of each column.

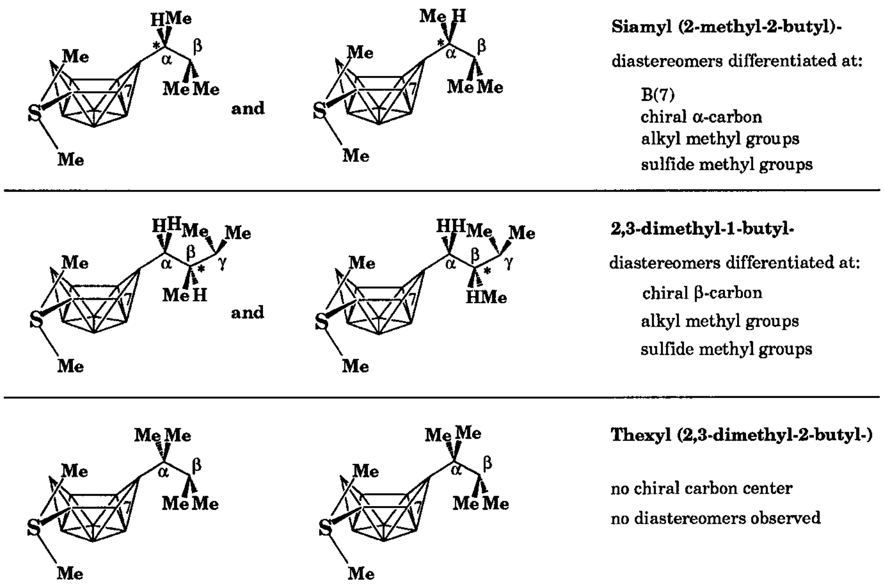

Figure 1. Diastereomers observed for various derivatives and correlation to the pattern of resonances observed for their ^{13}C NMR spectra.

addition of a cluster B−H bond to the olefin, and the relocation of the remaining Me_2S group to the B(8 or 10) position. As the stable, unsubstituted 8-Se_2S-$B_{10}H_{12}$ forms only at elevated temperatures in the absence of olefin, the Me_2S loss during in the present case must be closely coupled to the hydroboration of the olefin. As 8-SMe_2-$B_{10}H_{12}$ fails to hydroborate olefins, even at high temperatures,[11] it is likely that 8-SMe_2-$B_{10}H_{12}$ forms via isomerization of a reactive Me_2S-$B_{10}H_{12}$ isomer that also undergoes hydroboration to the 6-R-8-SMe_2-$B_{10}H_{11}$. How or why the remaining Me_2S group ends up in the asymmetric B(8 or 10) position in both 8-SMe_2-$B_{10}H_{12}$ and substituted 6-R-8-SMe_2-$B_{10}H_{11}$ species is not known.

The ^{11}B spectrum of 6-Thx-$B_{10}H_{13}$ displays the anticipated symmetry and intensities. The singlet at +27.6 ppm corresponds to the Thx-B(6) atom. ^{11}B−^{11}B COSY NMR provides an unambiguous assignment of all resonances, and all expected cross-couplings are observed. The chemical shift environments of the various resonances correspond to a typical *nido* system. ^{11}B NMR spectra of 6-R-$B_{10}H_{13}$ derivatives appear to be largely solvent independent, except for a slight substituent dependence in both the B(6) and B(9) signals. The ^{11}B, ^{1}H, and ^{13}C NMR data for 6-Thx-$B_{10}H_{13}$ are presented in Table 4. The thexyl and siamyl groups were chosen as models because of their steric properties and the relative simplicity of their proton spectra, compared to those of longer, straight-chain aliphatics. Examination of the intensities and multiplicities of the ^{1}H NMR spectra together with the number and types of ^{13}C resonances deduced from DEPT-135 experiments indicated that only one alkyl isomer is present in each derivative, that of the anti-Markovnikov product. In addition, all the expected symmetry elements generated by a particular alkyl substituent were observed, indicating free rotation within the alkyl groups. All the ^{13}C spectra contain a broadened hump in the 20−25 ppm range corresponding to the carbon atom adjacent to the borane cage, a result of scaler coupling to the quadrupolar ^{11}B and ^{10}B nuclei.

Experimental Section

All reactions were performed under vacuum or in an atmosphere of dry nitrogen. Decaborane(14) and 6,9-$(SMe_2)_2$-$B_{10}H_{12}$ were obtained from laboratory stock. Alkenes were commercial samples, stored under N_2, and used as received. Li[Et_3BH] (Superhydride), Na[Et_3BH], and HCl/Et_2O were purchased from Aldrich and stored and transferred under nitrogen. NaH was washed repeatedly with dry hexanes and stored under N_2. $Me_4N[B_{10}H_{13}]$ was prepared by the addition of an Et_2O solution of $B_{10}H_{14}$ to an aqueous solution of Me_4NOH.[12] (It is essential to remove excess base and thoroughly dry the $Me_4N[B_{10}H_{13}]$.) MeLi, BuLi, and t-BuLi were purchased from Aldrich and transferred to nitrogen-filled storage bottles. Solvents were dried conventionally and distilled under nitrogen.

The ^{11}B NMR spectra were obtained using either a Brucker AM-500 or AM-360 spectrometer operating at 160.46 and 115.54 MHz, respectively. The ^{1}H NMR spectra were obtained on the same spectometers as well as Brucker WP-200, WP-270, AC^+-300, and AC^+-250 spectrometers, all at the model number frequencies. The ^{13}C NMR spectra were obtained using Brucker WP-270 at 68 MHz, AC^+-250 at 62.5 MHz, AC^+-300 at 75 MHz, AM-360 at 90 MHz, and AM-500 at 125 MHz.

Table 4. ^{11}B, ^{13}C, and ^{1}H NMR Data for 6-Thx-$B_{10}H_{13}$ (Coupling Constants in Parentheses)

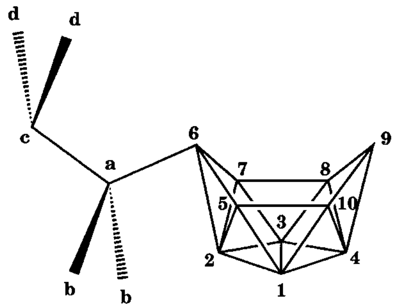

^{11}B NMR: 160 MHz, C_6D_6

B(6)	+27.6 s (–)	B(9)	-7.2 d (175)
B(1,3)	+9.7 d (147)	B(2)	-35.1 d (156)
B(5,7)	-4.2 d (151)	B(4)	-39.4 d (151)
B(8,10)	+0.2 d (155)		

^{13}C NMR 75MHz; C_6D_6

a)	+30.0	1C
c)	+39.9	1C
b) or	+26.3	2C
d)	+18.7	2C

^{1}H NMR 300MHz; C_6D_6

b)	+1.05	s	(–)	6H
c)	+1.30	sept.	(7)	1H
d)	+0.54	d	(7)	6H

A. Preparation of 6-*n*-Hex-8-SMe$_2$-B$_{10}$H$_{11}$. $B_{10}H_{12}\cdot 2SMe_2$, 1.027 g (4.21mmol), was dissolved in 30 mL of CH_2Cl_2 under N_2, and 6.878 g (81.9 mmol) of 1-hexene (98%) was injected with stirring. After 2 days of brisk stirring the solvent and excess olefin were removed under vacuum. Rotary chromatography of the residue using hexanes and then hexanes/CH_2Cl_2 (88:12) as the elutant gave 0.894 g (80% yield) of viscous oil product.

B. Preparation of 6-Thx-8-SMe$_2$-B$_{10}$H$_{11}$. $B_{10}H_{12}\cdot 2SMe_2$, 4.806 g (19.69 mmol), was dissolved in 30 mL of CH_2Cl_2. Then 4.637 g of 2,3-dimethyl-2-butene (98%) was injected with stirring. After 4 days of brisk stirring, the mixture was checked by ^{11}B NMR for completion, and then the solvent and excess olefin were removed under vacuum. Rotary chromatography of the residue using hexanes and then hexanes/CH_2Cl_2 (88:12) yielded 4.986 g (19.16 mmol, 97% yield) of product.

C. Preparation of 6-Pr-8-SMe$_2$-B$_{10}$H$_{11}$. $B_{10}H_{12}\cdot 2SMe_2$, 2.150 g (8.81 mmol), was dissolved in 35 mL of CH_2Cl_2 in a 250 mL vacuum flask. The system was freeze/thawed three times and evacuated. Then 26.23 mmol of propene was condensed into the solution at −196 °C. The system was closed and stirred for 4 days at room temperature, during which time the reaction was periodically sampled to check its progress. The solvent and excess olefin were then removed under vacuum, and the oily residue was purified via rotary chromatography, as above.

D. Preparation of 6-Oct-8-SMe$_2$-B$_{10}$H$_{11}$. $B_{10}H_{12}\cdot 2SMe_2$, 1.527 g (6.26 mmol), and an excess of 1-octene were dissolved in 30 mL of benzene. The system was refluxed for 3.5 h, after which time ^{11}B NMR analysis showed complete conversion to 6-Oct-8-SMe$_2$-B$_{10}$H$_{11}$. The benzene was evaporated and the product isolated by rotary chromatography using hexanes/CH_2Cl_2 (86:14) as above.

E. Conversion of 6-R-8-SMe$_2$-B$_{10}$H$_{11}$ to 6-R-B$_{10}$H$_{12}^{-}$. In a typical reaction, 4.16 mmol of 6-Sia-8-SMe$_2$-B$_{10}$H$_{11}$ was prepared from 2-methyl-2-butene (20.16 mmol) and 1.015 g (4.16 mmol) of $B_{10}H_{12}\cdot 2SMe_2$ in CH_2Cl_2. The solvent and excess olefin were evaporated in vacuum, and the residue was redissolved in CH_2Cl_2. Then 4.40 mL of 1 M Superhydride, $LiEt_3BH$/THF, was injected with stirring. The solution immediately turned bright yellow. ^{11}B NMR analysis showed two boron compounds present, 6-R-$B_{10}H_{12}^{-}$ and Et_3B. The solvent was again removed and the residue washed with several portions of hexanes to remove Et_3B. The product can be further purified following metathesis with tetraalkylammonium salts.

F. One-pot Preparation of 6-Thx-B$_{10}$H$_{13}$ via Hydroboration $B_{10}H_{12}\cdot 2SMe_2$, 2.247 g (9.21 mmol), was dissolved in 20 mL of dry CH_2Cl_2. Then 3.863 g of 2,3-dimethyl-2-butene (36.85 mmol) was injected with stirring. The reaction was allowed to stir briskly for 2 days. The solution was analyzed by ^{11}B NMR to ascertain the completeness of the reaction. The solvent and excess olefin were then removed under vacuum, and the residue was redissolved in CH_2Cl_2. Then 9.2 mL of 1.0 M $LiEt_3BH$ was injected with stirring. The pale yellow solution immediately turned bright yellow. After about 5 min 9.7 mL of 1.0 M HCl/Et_2O was injected with stirring. The solution quickly cleared with the formation of a white solid. ^{11}B NMR showed complete conversion to 6-R-$B_{10}H_{13}$. The solution was filtered to remove LiCl, and the solvents were removed under vacuum. Then the residue was dissolved in hexanes with enough CH_2Cl_2 to completely dissolve the residue. The solution was mounted on the rotary chromatograph, and the solvent was evaporated. The plate was then eluted with hexanes until a large broad band was completely removed. The fractions were combined and evaporated to give 1.605 g (7.79 mmol) of 6-Thx-$B_{10}H_{13}$ in an 84.6% yield. The viscous oil crystallized upon standing. Electron impact mass spectroscopy of 6-Thx-$B_{10}H_{13}$ yielded a parent peak $M^+ = m/z$ 206, and the thexyl group fragment at $M^+ = m/z$ 85.

G. Preparation of 6-R-B$_{10}$H$_{13}^{2-}$ via Na[B$_{10}$H$_{13}$] in Et$_2$O. In a typical reaction, 0.269 g (1.86 mmol) of Na[$B_{10}H_{13}$] was dissolved in 12 mL of Et_2O. The system was then cooled to −78 °C, and 2.0 mL of 1.4 M Et_2O solution of MeLi was injected dropwise with stirring. The mixture was warmed to room temperature, during which time the yellow color faded and a gelatinous precipitate formed. The solution was stirred for an additional 20 min at room temperature. ^{11}B NMR showed a dilute spectrum of 6-Me-$B_{10}H_{13}^{2-}$. The ether was removed and the product redissolved in THF. To this solution was added 1.546 g of [Ph_3PMe]Br dissolved in CH_2Cl_2. A voluminous red-orange precipitate immediately formed. The solid was filtered out and washed with THF. The precipitate was then extracted with CH_2Cl_2 to remove the NaBr and LiBr, leaving a dark-orange solution. The product was precipitated from this solution with Et_2O and dried *in vacuo* to give 0.864 g (1.25 mmol) of [Ph_3PMe]$_2$[6-Me-$B_{10}H_{13}$] in a 67% yield.

H. Preparation of 6-*n*-Bu-B$_{10}$H$_{13}^{2-}$ via R$_4$N[B$_{10}$H$_{13}$] in THF. Me_4N[$B_{10}H_{13}$], 0.485 g (2.48 mmol), was dissolved in 25 mL of THF, and the solution was cooled to −78 °C. Then 2.08 mL of 1.6 M BuLi was injected with stirring. Upon warming, the yellow color faded and a white precipitate formed. The sparingly soluble product was allowed to stir at room temperature for about 20 min. ^{11}B NMR of the mixture showed a spectrum consistent with a 6-R-$B_{10}H_{13}^{2-}$ species.

I. Protonation to 6-*n*-Bu-B$_{10}$H$_{14}^{-}$. To the THF solution formed in section **H** was injected 2.45 mL of 1.0 M HCl/Et_2O. The cloudy suspension cleared up somewhat, and then a white precipitate formed. ^{11}B NMR showed the formation of 6-*n*-Bu-$B_{10}H_{14}^{-}$.

J. One-Pot Preparation of 6-Me-B$_{10}$H$_{13}$ via RLi. To a 150 mL Et_2O solution of 1.230 g (8.54 mmol) of Na[$B_{10}H_{13}$] was injected 7.40 mL of 1.4 M MeLi in Et_2O at −78 °C. The yellow solution became colorless, and small amounts of precipitate formed. The system was slowly brought to room temperature. ^{11}B NMR analysis showed the formation of 6-Me-$B_{10}H_{13}^{2-}$. The system was then injected with 19.0 mL of 1.0 M HCl/Et_2O. The precipitate immediately dissolved, another precipitate formed, and gas evolution was observed. After 1.5 h of brisk stirring, ^{11}B NMR showed complete conversion to 6-R-$B_{10}H_{13}$ (and traces of 5-R-$B_{10}H_{13}$). The solvent and excess acid were removed at reduced pressure, and the residue was extracted several times with hexanes. The extracts were combined and filtered to remove LiCl and NaCl, and the solvent evaporated leaving 1.145 g of a yellow oil (98.6%). ^{11}B NMR analysis showed the presence of 6-Me-$B_{10}H_{13}$ (88.6%), $B_{10}H_{14}$ (3.1%), and an unidentified product (8.3%), giving an overall yield of 6-Me-$B_{10}H_{13}$ as 87.3%. The product was further purified by rotary chromatography using hexanes as elutant.

Acknowledgment. We thank the National Science Foundation for partial support of this research and for major departmental instrumentation grants.

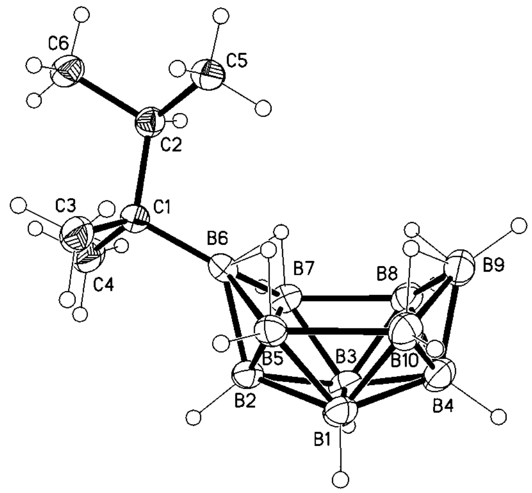

Figure 2. Crystallographically determined structure of 6-Thx-$B_{10}H_{13}$ (thermal probability ellipsoids drawn at the 50% probability level).

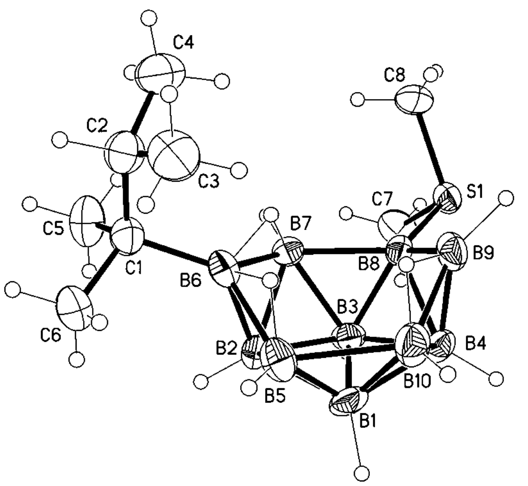

Figure 3. Crystallographically determined structure of 6-Thx-8-SMe_2-$B_{10}H_{12}$ (thermal probability ellipsoids drawn at the 50% probability level). The Thx group is disordered. Only the more fully occupied Thx group is shown.

Appendix

Crystal Structures of 6-Thx-$B_{10}H_{13}$, 6-Thx-8-SMe_2-$B_{10}H_{11}$, and 8-SMe_2-$B_{10}H_{11}$. Structural analyses of the isoelectronic *nido* decaborane derivatives 6-Thx-$B_{10}H_{13}$, 6-Thx-8-SMe_2-$B_{10}H_{11}$, and 8-SMe_2-$B_{10}H_{12}$, shown in Figures 2−4, indicate that the SMe_2 moiety has a greater impact on cluster geometry than the terminal alkyl group. This may be attributed to several interrelated factors: first, the increased electron donation of the sulfide relative to a terminal hydride; second, the reduction of the number of bridge hydrogens (as prescribed by Wade's rules) by one in 6-Thx-8-SMe_2-$B_{10}H_{11}$ and 8-SMe_2-$B_{10}H_{12}$ which results in unbridged B(8)−B(9). The subsequent contractions of the B(7)-B(8) and B(8)-B(9) connectivities in 6-Thx-8-SMe_2-$B_{10}H_{11}$ and in 8-SMe_2-$B_{10}H_{12}$ by ca. 10% result in a twisting of the cage framework where B(8) swings inward, dragging B(7) with it, while B(10) is pushed outward slightly . As a result, 6-Thx-8-SMe_2-$B_{10}H_{11}$ is distinctly distorted in the same way as 8-SMe_2-$B_{10}H_{12}$, rather than being intermediate between 8-SMe_2-$B_{10}H_{12}$ and 6-Thx-$B_{10}H_{13}$. Despite the presence of the sterically demanding thexyl group, the influence of the SMe_2 moiety dictates the major observed structural changes in 6-Thx-8-SMe_2-$B_{10}H_{11}$ and 8-SMe_2-$B_{10}H_{12}$. Tables 5 and 6 contain selected bond angles and distances to illustrate the points discussed. Additional data are in the Supporting Information. Crystals of 6-Thx-8-SMe_2-$B_{10}H_{11}$ were difficult to grow. The most suitable crystal had dimensions of 0.20 × 0.14 × 0.10 mm. This small crystal size and disorder in the thexyl side chain led to a structural result with large residues.

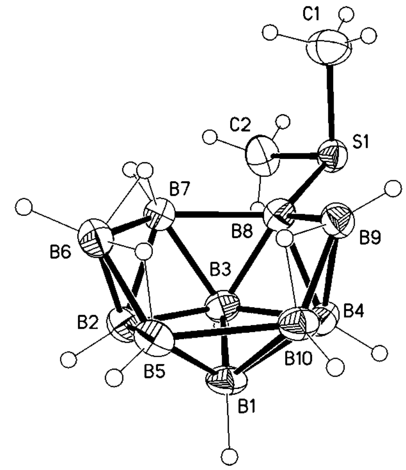

Figure 4. Crystallographically determined structure of 8-SMe_2-$B_{10}H_{12}$ (thermal probability ellipsoids drawn at the 50% probability level).

Table 5. Selected Bond Lengths (in Å) for the Species 6-Thx-$B_{10}H_{13}$, 6-Thx-8-SMe_2-$B_{10}H_{11}$, and 8-SMe_2-$B_{10}H_{12}$

bond	6-Thx-$B_{10}H_{13}$	6-Thx-8-SMe_2-$B_{10}H_{12}$	8-SMe_2-$B_{10}H_{12}$
1−10	1.747(3)	1.797(10)	1.783(6)
2−6	1.734(3)	1.737(9)	1.703(6)
3−8	1.748(3)	1.723(9)	1.722(6)
4−9	1.718(3)	1.765(10)	1.755(6)
5−6	1.811(2)	1.821(10)	1.776(6)
5−10	1.979(3)	2.063(10)	2.028(6)
7−8	1.981(3)	1.842(9)	1.833(5)
8−9	1.790(3)	1.657(9)	1.647(5)

Table 6. Selected Bond Angles (in deg) for the Species 6-Thx-$B_{10}H_{13}$, 6-Thx-8-SMe_2-$B_{10}H_{11}$, and 8-SMe_2-$B_{10}H_{12}$

angle	6-Thx-$B_{10}H_{13}$	6-Thx-8-SMe_2-$B_{10}H_{11}$	8-SMe_2-$B_{10}H_{12}$
10−1−3	107.98(14)	104.8(5)	106.1(3)
8−3−7	68.97(12)	63.1(4)	62.6(2)
7−3−4	117.9(2)	113.4(5)	111.6(3)
8−3−2	117.74(14)	113.4(5)	112.2(3)
9−4−3	111.23(14)	106.2(5)	106.3(3)
9−4−8	61.47(11)	55.4(4)	55.6(2)
8−4−10	104.89(14)	99.8(5)	100.3(3)
6−5−10	118.57(13)	113.5(5)	113.4(3)
6−7−8	117.92(13)	121.4(5)	121.8(3)
3−8−9	109.21(14)	113.8(5)	114.0(3)
4−8−9	57.51(11)	61.2(4)	61.5(2)
3−8−7	55.56(10)	60.4(4)	60.9(2)
4−8−7	106.70(13)	110.1(4)	110.2(3)

Supporting Information Available: Figures S1−S12, showing NMR spectra (^{11}B) of 6-R-$B_{10}H_{13}^{2-}$ (R = Me, CN), Me_4N[6-*n*-Bu-$B_{10}H_{14}$], 6-Thx-8-SMe_2-$B_{10}H_{11}$, 8-Se_2S-$B_{10}H_{12}$, 6-Sia-8-SMe_2-$B_{10}H_{11}$, and 6-Thx-$B_{10}H_{13}$, $^{11}B-^{11}B$ COSY NMR spectra of Na_2[6-CN-$B_{10}H_{13}$], Me_4N[6-*n*-Bu-$B_{10}H_{14}$], 8-SMe_2S-$B_{10}H_{12}$, and 6-Thx-$B_{10}H_{13}$. $^{13}C\{^1H\}$ NMR spectra of 6-Sia-$B_{10}H_{11}$, and 6-Thx-8-SMe_2-$B_{10}H_{11}$, and tables of X-ray experimental details and crystallographic data, all atomic coordinates, anisotropic thermal parameters, and bond distances and angles, and processing references for 6-Thx-$B_{10}H_{13}$, 6-Thx-8-SMe_2-$B_{10}H_{11}$, and 8-SMe_2-$B_{10}H_{12}$ (47 pages). Ordering information is given on any current masthead page.

IC971149N